

## SUPPORTING INFORMATION

### **Visualizing specific Cross-Protomer Interactions in the Homo-Oligomeric Membrane Protein Proteorhodopsin by DNP-enhanced Solid-state NMR**

Jakob Maciejko<sup>1</sup>, Michaela Mehler<sup>1</sup>, Jagdeep Kaur<sup>1</sup>,  
Tobias Lieblein<sup>2</sup>, Nina Morgner<sup>2</sup>, Olivier Ouari<sup>3</sup>, Paul Tordo<sup>3</sup>,  
Johanna Becker-Baldus<sup>1</sup> & Clemens Glaubitz<sup>1\*</sup>

- (1) Institute for Biophysical Chemistry & Centre for Biomolecular Magnetic Resonance, Goethe-University Frankfurt, Germany
- (2) Institute for Physical and Theoretical Chemistry, Goethe-University Frankfurt, Germany
- (3) Aix-Marseille Université, CNRS, ICR, UMR 7273, 13013 Marseille, France

(\*) Corresponding author.

Email: [glaubitz@em.uni-frankfurt.de](mailto:glaubitz@em.uni-frankfurt.de)

Institute of Biophysical Chemistry

Goethe University Frankfurt

Max-von-Laue-Str. 9

60438 Frankfurt am Main

Germany

Tel.: +49-69-798-29927

Fax.: +49-69-798-29929

## (A) Supporting optical data

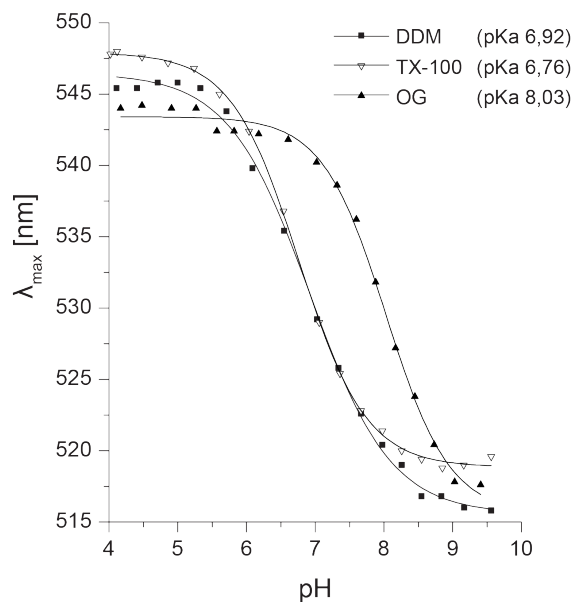


**Fig. S1: (a)** pKa values of the primary proton acceptor Asp97 of green PR in different detergents, determined by pH-titration experiments. Green PR in TX-100 shows a pKa at ~7, comparable to DDM as previously reported<sup>1,2</sup>. Solubilization in OG induces a considerable shift to a pKa at ~8, indicating some conformational impact of the detergent on the protein. To ensure more native conditions during mixed sample preparation, TX-100 was favoured as the oligomeric disruptor.

**(B) Statistics of mixed- labeled complexes**

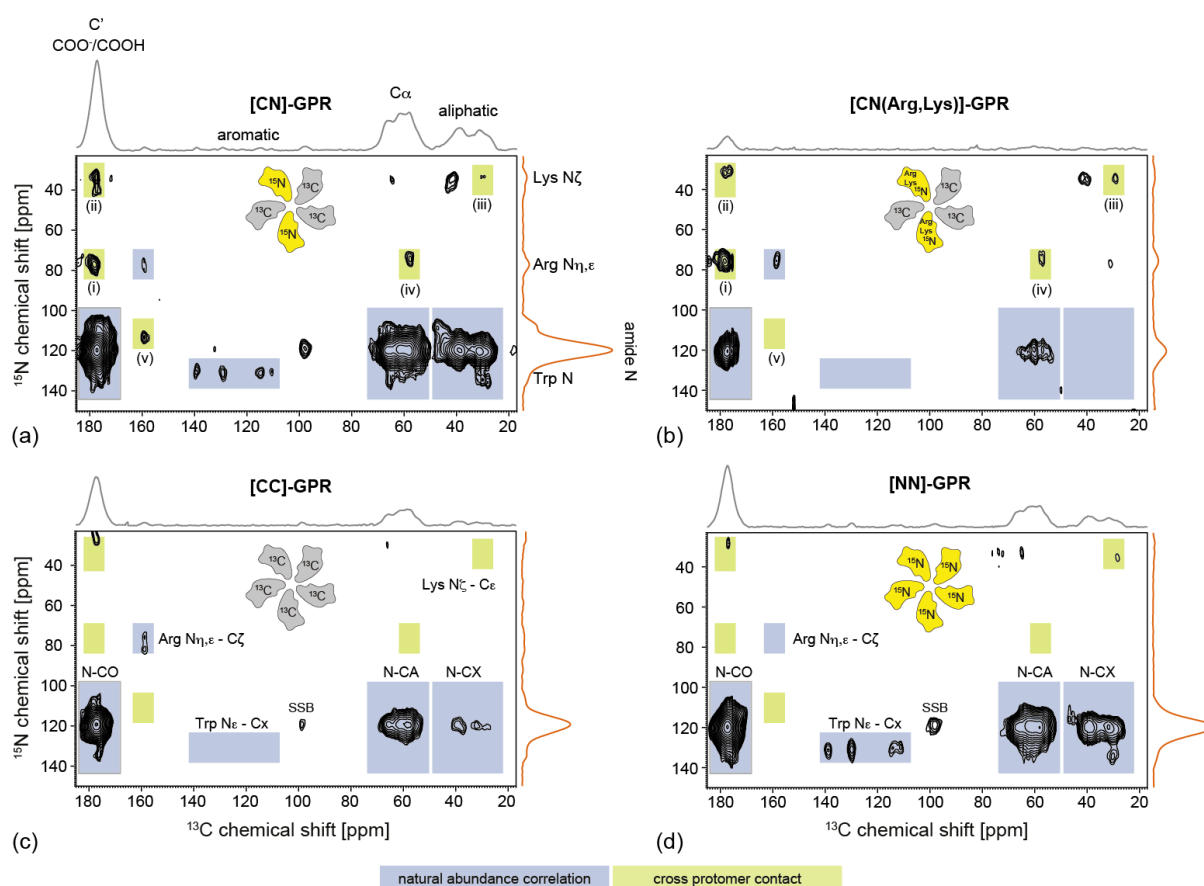
**Table. S1: Statistical analysis of pentamer and hexamer configuration and their population**

(N=size of the complex, k=number of differently labeled protomers within the complex, P=population, I=number of interfaces between <sup>13</sup>C- and <sup>15</sup>N-labeled protomers, I<sub>Unique</sub>=number of unique interfaces)

N	5							
k	0	1	2		3		4	5
P	1	5	10		10		5	1
			5	5	5	5		
I	0	2	4	2	4	2	2	0
I <sub>Unique</sub>	0	1	2	1	2	1	1	0
Average number of interfaces per complex:								
$I^{Avg} = \frac{\sum_{k=0}^5 P(5,k) \times I(5,k)}{\sum_{k=0}^5 P(5,k)} = \frac{(1 \times 0) + (5 \times 2) + (5 \times 4 + 5 \times 2) + (5 \times 4 + 5 \times 2) + (5 \times 2) + (1 \times 0)}{32} = \frac{80}{32} = 2.5$								
Average number of unique interfaces per complex:								
$I_{Unique}^{Avg} = \frac{\sum_{k=0}^5 P(5,k) \times I_{Unique}(5,k)}{\sum_{k=0}^5 P(5,k)} = \frac{(1 \times 0) + (5 \times 1) + (5 \times 2 + 5 \times 1) + (5 \times 2 + 5 \times 1) + (5 \times 1) + (1 \times 0)}{32} = \frac{40}{32} = 1.25$								

N	6													
k	0	1	2			3			4			5	6	
P	1	6	15			20			15			6	1	
			3	6	6	6	6	2	6	6	3			
I	0	2	4	4	2	2	4	4	6	2	4	4	2	0
I <sub>Unique</sub>	0	1	2	2	1	1	2	2	3	1	2	2	1	0
Average number of interfaces per complex:														
$I^{Avg} = \frac{\sum_{k=0}^6 P(6,k) \times I(6,k)}{\sum_{k=0}^6 P(6,k)} = \frac{(1 \times 0) + (6 \times 2) + (3 \times 4 + 6 \times 4 + 6 \times 2) + (6 \times 2 + 6 \times 4 + 6 \times 4 + 2 \times 6) + (6 \times 2 + 6 \times 4 + 3 \times 4) + (6 \times 2) + (1 \times 0)}{64} = \frac{192}{64} = 3.0$														
Average number of unique interfaces per complex:														
$I_{Unique}^{Avg} = \frac{\sum_{k=0}^6 P(6,k) \times I_{Unique}(6,k)}{\sum_{k=0}^6 P(6,k)} = \frac{(1 \times 0) + (6 \times 1) + (3 \times 2 + 6 \times 2 + 6 \times 1) + (6 \times 1 + 6 \times 2 + 6 \times 2 + 2 \times 3) + (6 \times 1 + 6 \times 2 + 3 \times 2) + (6 \times 1) + (1 \times 0)}{64} = \frac{96}{64} = 1.5$														

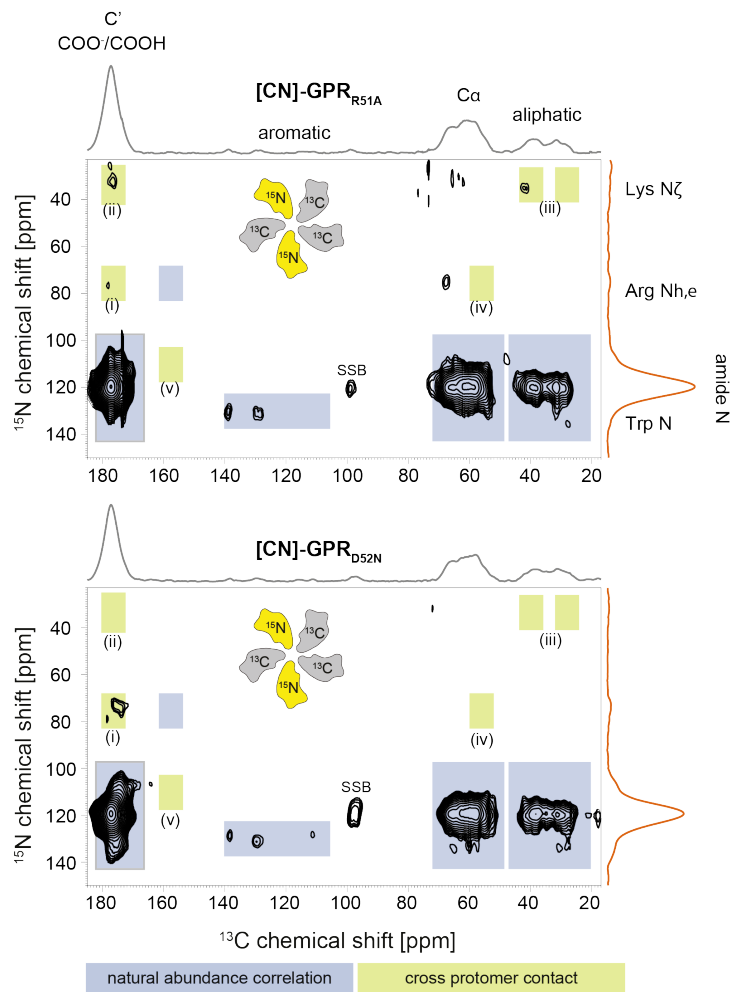
### (C) Supporting NMR data



**Fig. S2:** DNP-enhanced 2D-TEDOR spectra ( $t_{\text{mix}}=6.25\text{ms}$ ) of (a) [CN]-GPR, (b) [CN(Arg,Lys)]-GPR, (c) [CC]-GPR and (d) [NN]-GPR. The latter two control samples allow clear identification of natural abundance correlations. In [CC]-GPR,  $^{13}\text{C}$  has been enriched while  $^{15}\text{N}$  occurs at its natural abundance of 0.366%. In contrast, [NN]-GPR has been  $^{15}\text{N}$  enriched but  $^{13}\text{C}$  depleted by using  $^{12}\text{C}_6$ -glucose, so that the  $^{13}\text{C}$  natural abundance is reduced from 1.1% to 0.5%. Therefore,  $^{15}\text{N}$ - $^{13}\text{C}$  spin pairs occur between the naturally occurring and the enriched isotope species. Estimations are given in Tab. S2. For example, a pentamer in [NN]-GPR, [CC]-GPR and [CN]-GPR contains 6.8, 5.0 and 5.9 N-CA spin pairs, respectively (see Tab. S2). Due to the signal enhancement by DNP, strong N-CO, NCA and N-CX cross peaks between these enriched and naturally occurring isotopes are detected in both samples. The N-CX cross peaks in [CC]-GPR are smaller compared to [NN]-GPR due to stronger dipolar truncation of long-range contacts in the  $^{13}\text{C}$ -labelled samples and due to  $^{13}\text{C}$ - $^{13}\text{C}$  J-couplings<sup>3</sup>. Interestingly, intra-residue cross peaks between Trp-N $\epsilon$  and Trp-C $\alpha$  are larger in [NN]-GPR, while intra-residue cross peaks between Arg-N $\eta,\epsilon$  and Arg-C $\zeta$  are better seen in [CC]-GPR. The natural abundance pattern in [CN(Arg,Lys)]-GPR (b) is identical that observed [CC]-GPR (c) due to the U- $^{13}\text{C}$ -labelled protomers mixed with  $^{15}\text{N}$ -Arg-Lys-GPR. In contrast, the natural abundance pattern in [CN]-GPR is a superposition of (c) and (d). In addition, N-CX cross peaks could also arise from non-specific long-range cross-protomer contacts explaining the slightly larger N-CX intensity.

The identification of the natural abundance correlation pattern allows assigning the remaining resonances to long-range cross-protomer through-space contacts:

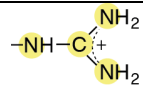
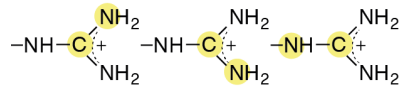
- (i): Contact between Arg-N $\eta,\epsilon$  - Asp- C $\gamma$ /Glu- C $\delta$
- (ii): Contact between Lys-N $\zeta$  - Asp- C $\gamma$ /Glu- C $\delta$
- (iii): Contact between Lys-N $\zeta$  and interface residues with aliphatic carbons, but also natural abundance contribution from Lys-N $\zeta$  - C $\epsilon$
- (iv): Contact between Arg-N $\eta,\epsilon$  and interface residues such as Ser or Thr
- (v): Contact between Arg-C $\zeta$  and other residues at the interface such as Gln/Asn or long-range contact to amide nitrogens.



**Fig. S3:** Full DNP-enhanced 2D-TEDOR spectra ( $t_{\text{mix}}=6.25\text{ms}$ ) of mixed single mutant samples [CN]-GPR<sub>R51A</sub> and [CN]-GPR<sub>D52N</sub> shown in Fig. 5d. Resonances (i)-(v) are described in Fig. S2.

**Table. S2: Estimation of  $^{13}\text{C}$ - $^{15}\text{N}$  spin pairs due to natural abundance**

The samples [NN]-GPR, [CC]-GPR and [CN]-GPR contain different levels of naturally occurring  $^{13}\text{C}$  and  $^{15}\text{N}$  isotopes, which create a certain number of spin pairs with the enriched isotope species causing cross peak pattern in  $^{15}\text{N}$ - $^{13}\text{C}$  TEDOR spectra. The natural abundance of  $^{15}\text{N}$  and  $^{13}\text{C}$  is 0.366% and 1.1%, respectively. Here, the  $^{13}\text{C}$  abundance has been reduced to 0.5% by using  $^{12}\text{C}_6$ -glucose. A mixed labeled [CN]-GPR sample therefore contains per pentamer e.g. approx. 6 x N-CO, 6 x N-CA and 0.2 x arginines, which carry both  $^{13}\text{C}$  and  $^{15}\text{N}$  isotopes in their guanidinium group.

Natural abundance spin pairs		[NN]-GPR 100% $^{15}\text{N}$ 0.5 % $^{13}\text{C}$	[CC]-GPR 0.366% $^{15}\text{N}$ 100 % $^{13}\text{C}$	[CN]-GPR
$^{15}\text{N}$ per monomer		275	1.01	138.0
$^{13}\text{CA}$ per monomer		1.37	275	138.2
$^{13}\text{CO}$ per monomer		1.37	275	138.2
$^{15}\text{N}$ - $^{13}\text{CA}$ per monomer/pentamer		1.37 / 6.87	1.01 / 5.03	1.19 / 5.93
$^{15}\text{N}$ - $^{13}\text{CO}$ per monomer/pentamer		1.37 / 6.87	1.01 / 5.03	1.19 / 5.93
$^{15}\text{N}$ -Arg per monomer / pentamer		15 / 75 <sup>(1)</sup>	0.05 / 0.27 <sup>(2)</sup>	7.5 / 37.6
$^{13}\text{C}$ -Arg per monomer / pentamer		0.02 / 0.12	5 / 25	2.5 / 12.6
$^{13}\text{C}$ - $^{15}\text{N}$ -Arg per pentamer		0.12	-	0.06
		-	0.27	0.14

(1) Contains three  $^{15}\text{N}$  in the guanidinium group.

(2) Contains at least one  $^{15}\text{N}$  in the guanidinium group.

## (E) Characterization of green PR mutants

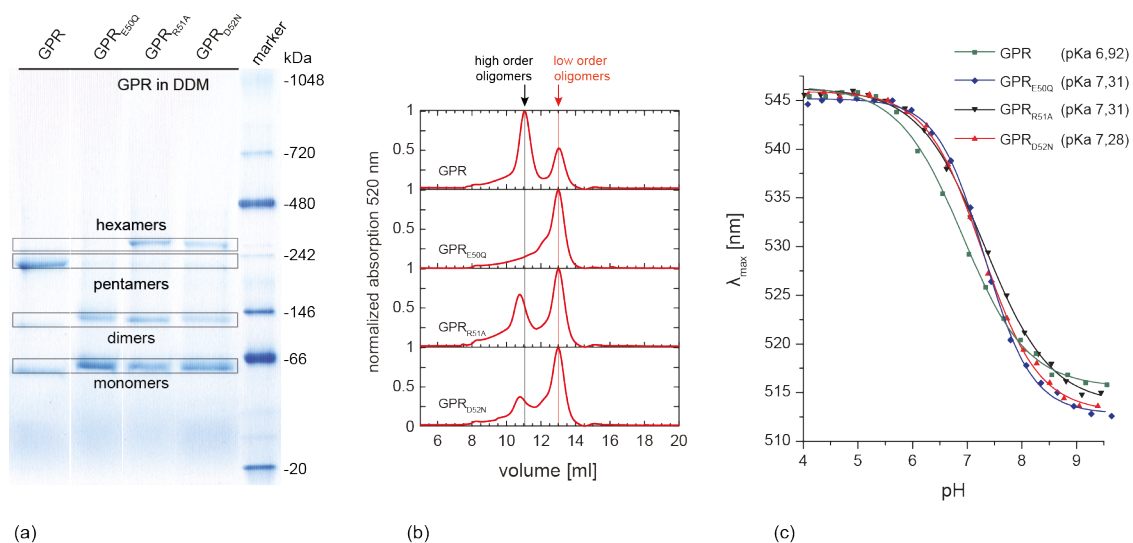


**Fig. S4:** (a) BN-PAGE analysis of green PR and its mutants E50Q, R51A and D52N in DDM. (b) Size exclusion chromatography of green PR and its mutants in DDM. GPR<sub>E50Q</sub> displays absence of the high order oligomer peak. GPR<sub>R51A</sub> and GPR<sub>D52N</sub> show a slight shift of the high order oligomer peak, indicating a larger hexameric state. These data agree with BN-PAGE in (a). (c) pKa values of the primary proton acceptor Asp97 of green PR single mutants in DDM, determined by pH-titration of their optical spectra.

### (E) Estimating the distance between R51 and D52

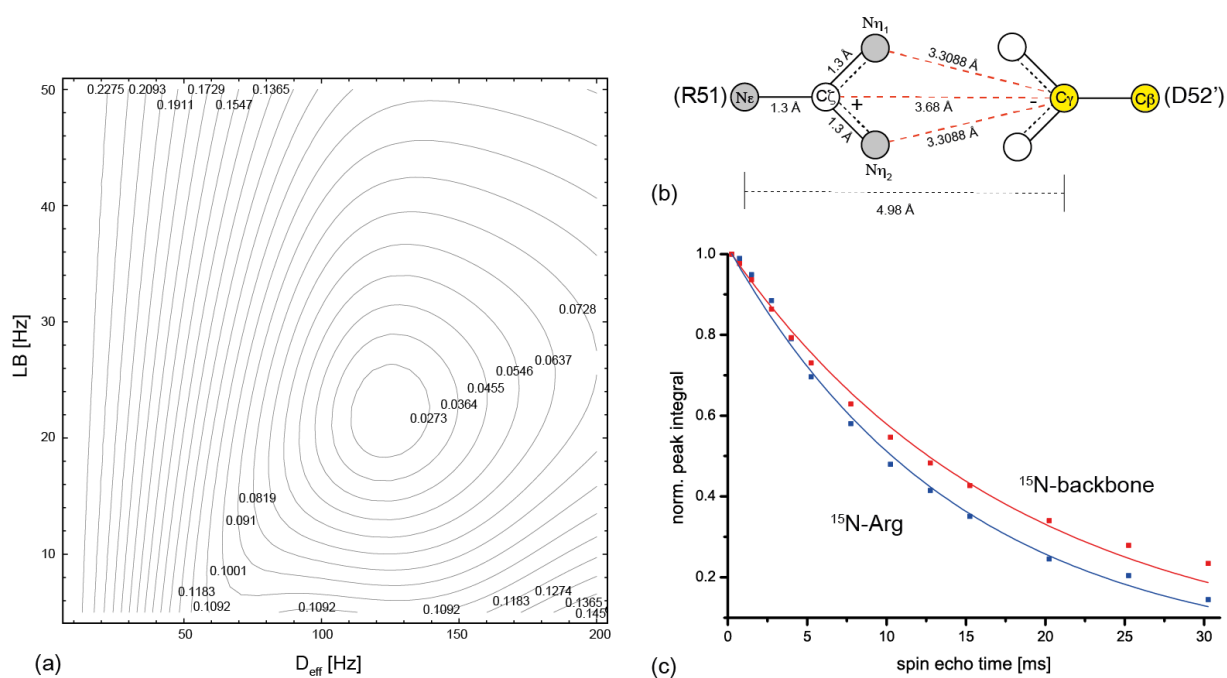


**Fig. S5:** (a) RMSD contour plot for the data shown in Fig. 6b. (b) Hypothetical linear arrangement of R51 and D52' resulting in an effective dipole coupling of 123 Hz. (c) As an additional control,  $^{15}\text{N}$ -T2' has been measured under conditions identical to the TEDOR experiment using a rotor-synchronized spin-echo after the cross polarization step. A value of  $(14.5 \pm 0.4)$  ms is obtained for the Arg-resonance corresponding to a linewidth of 22 Hz, which is in excellent agreement with the value extracted from the TEDOR buildup curve. For the backbone, a value of  $(17.8 \pm 0.5)$  ms is obtained.

**Table. S3: Cross-protomer salt bridges in crystal structures of blue PR<sup>4</sup>**

For comparison, distances between Arg-C $\zeta$ , N $\epsilon$ , N $\eta$ 1, N $\eta$ 2 and Asp-C $\gamma$  have been extracted and translated into <sup>13</sup>C-<sup>15</sup>N dipole couplings. From these values, the effective dipole coupling D<sub>eff</sub> has been calculated according to Eq. 3.

<b>Pentamer BPR<sub>D97N</sub> (HOT75m), PDB: 4KLY, (2.7 Å resolution)</b> Internuclear distances in R51-D52' salt bridges (Å) and corresponding <sup>13</sup> C- <sup>15</sup> N dipole couplings (Hz)					
C $\zeta$ -C $\gamma$	4.2	4.1	4.4	4.2	3.9
N $\epsilon$ -C $\gamma$	5.6 (17.4)	5.4 (19.4)	5.1 (23.1)	5.5 (18.4)	5.2 (21.8)
N $\eta$ 1-C $\gamma$	3.8 (55.8)	3.7 (60.5)	3.1 (102.8)	3.7 (60.5)	3.5 (71.4)
N $\eta$ 2-C $\gamma$	3.7 (60.5)	3.5 (71.4)	5.2 (21.8)	3.7 (60.5)	3.5 (71.4)
D <sub>eff</sub>	84.1	95.6	107.5	87.4	103.4
average D <sub>eff</sub>	95.8 Hz				

<b>Pentamer BPR<sub>D97N,Q105L</sub> (HOT75m), PDB: 4KNF, (2.6 Å resolution)</b> Internuclear distances in R51-D52' salt bridges (Å) and corresponding <sup>13</sup> C- <sup>15</sup> N dipole couplings (Hz)					
C $\zeta$ -C $\gamma$	4.0	4.2	4.3	3.9	4.3
N $\epsilon$ -C $\gamma$	5.3 (20.5764)	5.1 (23.1)	5.7 (16.5)	5.2 (21.8)	5.0 (24.5)
N $\eta$ 1-C $\gamma$	3.8 (55.8273)	2.9 (125.6)	4.0 (47.8)	3.4 (77.9)	3.0 (113.5)
N $\eta$ 2-C $\gamma$	3.3 (85.2424)	5.0 (24.5)	3.7 (60.5)	3.5 (71.4)	5.1 (23.1)
D <sub>eff</sub>	103.9	130.0	78.8	107.9	118.4
average D <sub>eff</sub>	108.0 Hz				

<b>Hexamer BPR (Med12BPR), PDB: 4JQ6, (2.31 Å resolution)<sup>(*)</sup></b> Internuclear distances in R33-D35' salt bridges (Å) and corresponding <sup>13</sup> C- <sup>15</sup> N dipole couplings (Hz)		
C $\zeta$ -C $\gamma$	4.4	4.3
N $\epsilon$ -C $\gamma$	5.6 (17.4)	5.6 (18.4124)
N $\eta$ 1-C $\gamma$	3.7 (60.5)	3.7 (60.4773)
N $\eta$ 2-C $\gamma$	4.4 (35.9)	4.0 (47.8649)
D <sub>eff</sub>	72.4	79.3
average D <sub>eff</sub>	75.8 Hz	

(\*) PDB file only contains 3 protomers, therefore only two sets of distances are given.

## (F) Influence of lipid and reconstitution conditions on the oligomerisation behavior of green PR

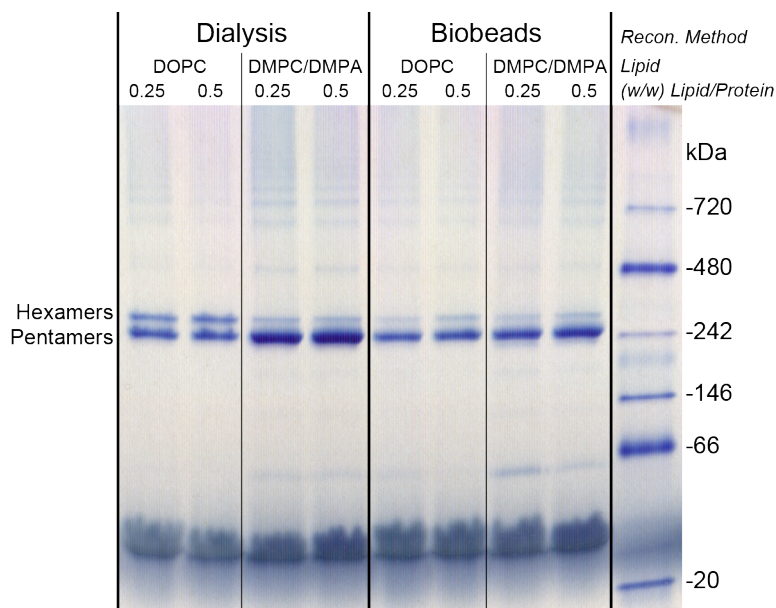


**Fig. S6:** BN-PAGE oligomerization analysis of green PR in proteoliposomes, reconstituted under different conditions. Slow detergent removal via dialysis and reconstitution into DOPC results in a high ratio of hexamers. This procedure has been reported in the past to lead to 2D crystals, which were analyzed by electron microscopy and AFM-imaging<sup>5,6</sup>. Both hexamers and pentamers are observed by AFM and BN-PAGE in DOPC under conditions close to those used for 2D crystallization. The lipid/protein ratio does not seem to affect the formation of hexamers. In contrast, dialysis into DMPC/DMPA proteoliposomes results in a much higher fraction of pentamers. Furthermore, mainly pentamers are observed when fast detergent removal is performed by Biobeads. The oligomeric state of reconstituted green PR is therefore independent of the lipid composition or the lipid/protein ratio. Hexamer formation seems to be specifically linked to 2D crystallisation.

### References

- (1) Friedrich, T.; Geibel, S.; Kalmbach, R.; Chizov, I.; Engelhard, M.; Bamberg, E. *Biophys. J.* **2002**, *82*, 228A.
- (2) Hempelmann, F.; Holper, S.; Verhoefen, M. K.; Woerner, A. C.; Kohler, T.; Fiedler, S. A.; Pflieger, N.; Wachtveitl, J.; Glaubitz, C. *J. Am. Chem. Soc.* **2011**, *133*, 4645.
- (3) Jaroniec, C. P.; Filip, C.; Griffin, R. G. *J. Am. Chem. Soc.* **2002**, *124*, 10728.
- (4) Ran, T.; Ozorowski, G.; Gao, Y.; Sineshchekov, O. A.; Wang, W.; Spudich, J. L.; Luecke, H. *Acta Crystallogr D* **2013**, *69*, 1965.
- (5) Klyszejko, A. L.; Shastri, S.; Mari, S. A.; Grubmuller, H.; Muller, D. J.; Glaubitz, C. *J. Mol. Biol.* **2008**, *376*, 35.
- (6) Shastri, S.; Vonck, J.; Pflieger, N.; Haase, W.; Kuehlbrandt, W.; Glaubitz, C. *Biochim. Biophys. Acta* **2007**, *1768*, 3012.